Acta Crystallographica Section B
**Structural Science**
ISSN 0108-7681

# Concomitant polymorphic behavior of di-$\mu$-thiocyanato-$\kappa^2N$:$S$;$\kappa^2S$:$N$-bis[bis(tri-*p*-fluorophenylphosphine-$\kappa P$)silver(I)]

**Bernard Omondi and Reinout Meijboom***

Department of Chemistry, University of Johannesburg, PO Box 524, Auckland Park 2006, Johannesburg, South Africa

Correspondence e-mail: rmeijboom@uj.ac.za

Received 9 June 2009
Accepted 16 November 2009

The structures of two polymorphs, both monoclinic $P2_1/n$ [polymorph (I)] and $P2_1/c$ [polymorph (II)], of di-$\mu$-thiocyanato-$\kappa^2N$:$S$;$\kappa^2S$:$N$-bis[bis(tri-*p*-fluorophenylphosphine-$\kappa P$)silver(I)] complexes have been determined at 100 K. In both polymorphs the complex has a dinuclear structure where the silver(I) coordinates to two phosphine ligands and two bridging thiocyanate anions to form complexes with distorted tetrahedral geometry. Polymorph (I) has just one half of the $[Ag_2(SCN)_2\{P(4\text{-}FC_6H_4)_3\}_4]$ molecule at (0, $\frac{1}{2}$, 0) from the origin in the asymmetric unit. Polymorph (II) has one and a half molecules of $[Ag_2(SCN)_2\{P(4\text{-}FC_6H_4)_3\}_4]$ in the asymmetric unit; the half molecule is situated at (0, 1, $\frac{1}{2}$), while the full molecule is located at (1/3, $\frac{1}{2}$, 1/3) from the origin. The Ag—P bond distances range from 2.4437 (4) to 2.4956 (7) Å in both polymorphs. The Ag—S distances are 2.5773 (7) Å in (I) and 2.5457 (5), 2.5576 (5) and 2.5576 (5) Å in (II). The full molecule in polymorph (II) has slightly shorter Ag—N bond distances [2.375 (1) and 2.367 (2) Å] compared with the half molecules in both polymorphs [2.409 (2) Å in (II) and 2.395 (2) Å in (I)]. The two polymorphs are compared using r.m.s. overlay calculations as well as half-normal probability plot analysis.

## 1. Introduction

Silver(I) complexes of the type $[AgL_nX]$ ($L$ is a tertiary phosphine or arsine, $n$ = 1–4 and $X$ is a coordinating or non-coordinating anion) were first prepared by Mann *et al.* (1937) and were the first crystallographic examples of metal phosphine complexes. These complexes are known to adopt a variety of geometries and nuclearities with different counterions and different ratios of phosphine (or other group 15 elements) ligands (Meijboom *et al.*, 2009), and can crystallize in different polymorphic forms, a phenomenon that was discussed previously (Venter, Roodt & Meijboom, 2009), showing the extreme differences such as 'cubic' (Teo & Calabrese, 1976*a*) or 'step' tetramers (Teo & Calabrese, 1976*b*). The environments of molecules in the crystals of polymorphic structures are often different and have an effect on the geometry of metal complexes (Hansson *et al.*, 2008). This can easily be studied in cases where one of the polymorphs has more than one molecule in the asymmetric unit (Hansson *et al.*, 2008). Previous studies were performed on the roles played by different properties of ligands during the crystallization of simple silver(I) salts with Group 15 donor ligands, with the initial focus on tri-*p*-tolylphosphine complexes (Meijboom *et al.*, 2006; Meijboom, 2006, 2007; Meijboom & Muller, 2006; Venter *et al.*, 2006; Venter, Roodt & Meijboom, 2009; Venter, Meijboom & Roodt, 2009) which

allowed for comparison with the isosteric triphenylphosphine complexes.

As a continuation of the above study and in addition to the previously studied di-$\mu$-thiocyanato-bis[bis(tri-*p*-tolyl)silver(I)] (Venter *et al.*, 2007) we present the crystal structures of two polymorphs of the title compound, di-$\mu$-thiocyanato-$\kappa^2N$:*S*;$\kappa^2S$:*N*-bis[bis(tri-*p*-fluorophenylphosphine-$\kappa P$)silver(I)], of which only five related examples can be found in the literature [Cambridge Structural Database (CSD), Version 5.30, May 2009 update; Allen, 2002]. The difference in geometric structures of the two polymorphs is analysed using r.m.s. overlay calculations as well as half-normal probability plots (Albertsson & Schultheiss, 1974; De Camp, 1973; Abrahams & Keve, 1971). The two structures are also compared with four other structures from the CSD; $[Ag_2(SCN)_2\{P(4\text{-}MeC_6H_4)_3\}_4]\cdot CH_3CN$ (Venter *et al.*, 2007), $[Ag_2(SCN)_2(PPh_3)_4]$ (Howatson & Morosin, 1973; Bowmaker *et al.*, 1997) and the two polymorphs of $[Ag_2(SCN)_2(PPh_2Cy)_4]$ (Effendy *et al.*, 2005).

Rapid ligand-exchange reactions have been reported for all NMR investigations of ionic monodentate phosphine complexes, thus making NMR spectroscopy of limited use for the characterization of these types of complexes (Muetterties & Alegranti, 1972).


**Figure 1**
Crystals of the two polymorphic forms: (*a*) cuboid crystals of size 0.22 × 0.15 × 0.05 mm of form (I) and (*b*) rhombohedral crystals of size 0.17 × 0.20 × 0.07 mm of form (II).

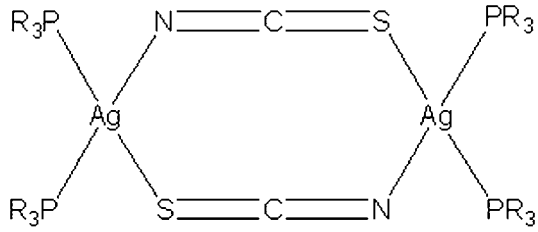


R = 4-$FC_6H_4$
(I)

## 2. Experimental

### 2.1. Synthesis

The title compounds were synthesized by heating one equivalent of $P(4\text{-}FC_6H_4)_3$ (0.335 g, 1.06 mmol) with AgSCN (0.176 g, 1.06 mmol) in acetonitrile (10.0 ml) under reflux. Recrystallization from acetonitrile produced colourless crystals suitable for X-ray diffraction in quantitative yield (0.410 g, 97.1%). The melting ranges (differential scanning calorimetry, DSC) of the two polymorphs are 451–454 K for (I) and 457–458 K for (II).

### 2.2. Crystallography and calculations

Crystals of (I) and (II) were grown from acetonitrile at room temperature. Single-crystal X-ray diffraction data were collected on a Bruker X8 Apex II 4K Kappa CCD diffractometer using Mo $K\alpha$ (0.71073 Å) radiation with $\varphi$ and $\omega$ scans at 100 (2) K. The initial unit-cell determination and data collection were achieved by the *APEX*2 (Bruker, 2005) software utilizing *COSMO* (Bruker, 2003) for the optimum collection of more than a hemisphere of reciprocal space. All reflections were merged and integrated using *SAINT* (Bruker, 2004) and were corrected for Lorentz, polarization and absorption effects using *SADABS* (Bruker, 2004). The structures were solved using *SIR*97 (Altomare *et al.*, 1999) and refined through full-matrix least-squares cycles using the *SHELXL*97 (Sheldrick, 2008) software package with $\Sigma(|F_o| - |F_c|)^2$ being minimized. All non-H atoms were refined with anisotropic displacement parameters.

Aromatic H atoms were placed in geometrically idealized positions [C—H = 0.93 Å for the $P2_1/c$ polymorph and 0.95 Å for polymorph (I)] and constrained to ride on their parent atoms, with $U_{iso}(H) = 1.2U_{eq}(C)$. For polymorph (II) the deepest residual electron-density hole (−0.66 e Å$^{-3}$) is located 0.67 Å from Ag, and the highest peak (0.61 e Å$^{-3}$) 0.69 Å from C223, whereas for (I) the deepest residual electron-density hole (−0.77 e Å$^{-3}$) is located 0.39 Å from Ag2, and the highest peak (0.0.47 e Å$^{-3}$) 0.76 Å from C215. Crystal data and details of data collection and refinement are given in Table 1.[1]

[1] Supplementary data for this paper are available from the IUCr electronic archives (Reference: ZB5008). Services for accessing these data are described at the back of the journal.

**Table 1**
Crystal data and structural refinement for (I) and (II).

For all structures: $C_{74}H_{48}Ag_2F_{12}N_2P_4S_2$, $M_r$ = 1596.88. Experiments were carried out at 100 K with Mo $K\alpha$ radiation using a Bruker SMART CCD area-detector diffractometer. Refinement was with 0 restraints. H-atom parameters were constrained.

| | (I) | (II) |
|---|---|---|
| Crystal data | | |
| Crystal system, space group | Monoclinic, $P2_1/n$ | Monoclinic, $P2_1/c$ |
| $a, b, c$ (Å) | 8.7406 (3), 15.4925 (6), 24.5352 (10) | 18.5885 (15), 14.0668 (12), 38.275 (3) |
| $\beta$ (°) | 91.2000 (10) | 96.551 (4) |
| $V$ (Å$^3$) | 3321.7 (2) | 9942.9 (14) |
| $Z$ | 2 | 6 |
| $D_x$ (Mg m$^{-3}$) | 1.597 | 1.6 |
| $\theta$ range (°) for cell measurement | 1.7–28.3 | 1.1–28.4 |
| $\mu$ (mm$^{-1}$) | 0.83 | 0.83 |
| Crystal shape | Cuboid | Rhombohedral |
| Crystal size (mm) | 0.26 × 0.2 × 0.1 | 0.4 × 0.36 × 0.32 |
| Data collection | | |
| Absorption correction | Multi-scan | Multi-scan |
| $T_{min}$, $T_{max}$ | 0.813, 0.922 | 0.732, 0.776 |
| No. of measured, independent and observed [$I > 2\sigma(I)$] reflections | 30 208, 8264, 6764 | 149 189, 24 770, 21 855 |
| $R_{int}$ | 0.052 | 0.032 |
| Range of $h, k, l$ | $h = -7 \rightarrow 11$, $k = -20 \rightarrow 19$, $l = -32 \rightarrow 32$ | $h = -24 \rightarrow 24$, $k = -18 \rightarrow 18$, $l = -51 \rightarrow 51$ |
| Refinement | | |
| $R[F^2 > 2\sigma(F^2)]$, $wR(F^2)$, $S$ | 0.037, 0.096, 1.05 | 0.026, 0.071, 1.09 |
| No. of reflections | 8264 | 24 770 |
| No. of parameters | 433 | 1297 |
| $\Delta\rho_{max}$, $\Delta\rho_{min}$ (e Å$^{-3}$) | 0.61, −0.66 | 0.47, −0.77 |

Computer programs: *APEX*2 (Bruker, 2005), *SAINT-Plus* and *XPREP* (Bruker, 2004), *SHELXS*97 and *SHELXL*97 (Sheldrick, 2008), *DIAMOND*3.0c (Brandenburg & Putz, 2004), *WinGX* (Farrugia, 1999).

All structures were checked for solvent-accessible cavities using *PLATON* (Spek, 1990) and the graphics were created with the *DIAMOND* (Brandenburg & Putz, 2005) Visual Crystal Structure Information System software. The r.m.s. calculations were performed with *HyperChem* (Hypercube Inc., 2002). Data for the half-normal probability plots were processed using *EXCEL*2003 (Microsoft, 2003).

### 2.3. DSC and hot-stage microscopy

DSC measurements were carried out using a Mettler–Toledo Star DSC 822 instrument. Small amounts (5–10 mg) of sample were weighed in aluminium pans and placed in the sample chamber of the calorimeter. The powders were then heated in the temperature range 303–523 K at a heating rate of 10 K min$^{-1}$ under ambient atmosphere.

Crystals were observed on a LINKAM LTS350 heating stage controlled by a LINKAM TP94 Heater/Cooler, mounted on a MOTIC BA300 polarizing microscope. Crystals were placed between two circular slides separated by metallic rings and heated/cooled at a rate of 10 K min$^{-1}$.

## 3. Results and discussion

### 3.1. Thermal analysis

$[Ag_2(SCN)_2\{P(4\text{-}FC_6H_4)_3\}_4]$ exists in two polymorphic forms that are easily identified by their crystal forms [polymorph (I) being cuboid and (II) being rhombic] as shown in Fig. 1. The thermal behaviour of these two polymorphic forms of $[Ag_2(SCN)_2\{P(4\text{-}FC_6H_4)_3\}_4]$ was analysed using DSC. The two polymorphic forms of $[Ag_2(SCN)_2\{P(4\text{-}FC_6H_4)_3\}_4]$ were not easily separated and as such the samples used for thermal studies were contaminated with small amounts of the other polymorph. A DSC study of each polymorph was started by increasing the temperature from 298 to 523 K. Fig. 2 contains the DSC traces of polymorph (I) and polymorph (II) during the first heating cycle and Table 2 reports the respective thermodynamic data. The traces of both polymorphs showed large endotherms at 386.75 and 402.90 K. The energies related to these two endotherms are relatively high compared with the heats of fusion for the two polymorphs. Dimeric structures $[Ag_2X_2L_2]$ have previously been described as partially separated monomers (Bowmaker *et al.*, 1996). We propose a similar behaviour for $[Ag_2(SCN)_2\{P(4\text{-}FC_6H_4)_3\}_4]$ in the solid state.[2] No visible change, however, is observed for this transition under the optical microscope – both polymorphs are unchanged until

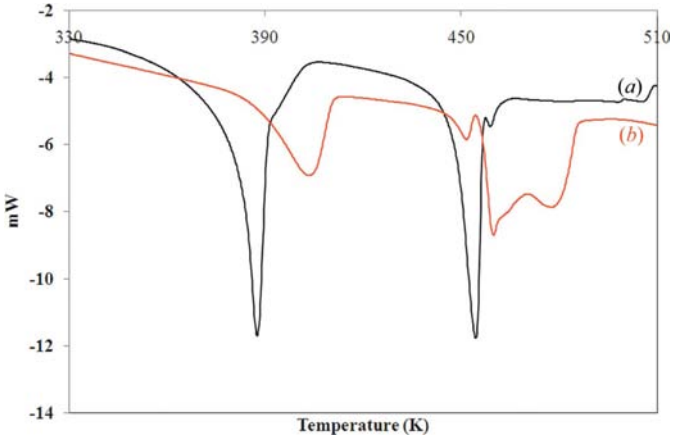


**Figure 2**
An overlay of the DSC traces for the two polymorphs, (*a*) polymorph (I) with traces of (II) and (*b*) polymorph (II) with traces of (I).

[2] We have observed similar behaviour for other dimeric silver phosphine complexes and are currently involved in an in-depth investigation of this phenomenon.

**Table 2**
Thermodynamic data obtained from DSC curves of $[Ag_2(NCS)_2(4\text{-}FC_{18}H_{12}P)_4]$ polymorphic forms.

| Polymorph | $T_{trs}$ (K) | $\Delta_{trs}H$ (kJ mol$^{-1}$) | $T_{fus}$ (K) | $\Delta_{fus}H$ (kJ mol$^{-1}$) | $T_{fus}$ (K) | $\Delta_{fus}H$ (kJ mol$^{-1}$) |
|---|---|---|---|---|---|---|
| (I) | 386.8 | −110.3 | 453.6 | −48.8 | 458.6 | −0.5 |
| (II) | 402.9 | −40.6 | 451.1 | −4.3 | 458.9 | −18.1 |

**Table 3**
Selected geometric parameters of (I) and (II) and for related structures (Å, °).

| | (I)[a] | (II*A*)[a] | (II*B*)[a] | (III)[b] | (IV)[b] | (V)[c] | (VI)[d] |
|---|---|---|---|---|---|---|---|
| Space group | $P2_1/n$ | $P2_1/c$ | | $P\bar{1}$ | $P2_1/c$ | $P\bar{1}$ | $P\bar{1}$ |
| Ag—P | 2.4560 (2) | 2.4437 (4) | 2.4534 (4) | 2.458 (1) | 2.372 (3) | 2.489 (1) | 2.5091 (8) |
| Ag—P | 2.4956 (7) | 2.4858 (5) | 2.4901 (4) | 2.437 (1) | 2.529 (2) | 2.454 (1) | 2.4612 (7) |
| Ag—P | – | 2.4485 (4) | – | – | – | – | – |
| Ag—P | – | 2.4907 (4) | – | – | – | – | – |
| Ag—N | – | 2.3750 (14) | – | – | – | – | – |
| Ag—N | 2.395 (2) | 2.3665 (14) | 2.4090 (15) | 2.336 (4) | 2.429 (8) | 2.343 (3) | 2.363 (3) |
| Ag—S | – | 2.5576 (5) | – | – | – | – | – |
| Ag—S | 2.5773 (7) | 2.5662 (5) | 2.5457 (5) | 2.667 (1) | 2.614 (3) | 2.581 (1) | 2.5955 (9) |

References: (*a*) this work; (*b*) Effendy *et al.* (2005); (*c*) Bowmaker *et al.* (1997); (*d*) Venter *et al.* (2007).

their melting points. Both changes are irreversible and no corresponding peaks were observed during the cooling cycles.

### 3.2. Molecular and crystal structures of (I) and (II)

The two polymorphs of the title compound have similar molecular geometry and crystallize to form dinuclear silver(I) complex molecules (Figs. 3 and 4). Polymorph (I) has only half a molecule of the complex in the asymmetric unit, whereas (II) has one and a half molecules in its asymmetric unit. The two $Ag^I$ atoms are bridged by two S═C═N$^-$ anions to form an eight-membered metallocycle. Examples of similar complexes from the literature include $[\{P(4\text{-}MeC_6H_4)_3\}_2Ag(SCN)_2Ag\{P(4\text{-}MeC_6H_4)_3\}_2]\cdot 2CH_3CN$ (VI) (Venter *et al.*, 2007) and $[(PPh_3)_2Ag(SCN)_2Ag(PPh_3)_2]$ (V) (Bowmaker *et al.*, 1997). The structures are also comparable to the two polymorphic forms made from 1,6-bis(diphenylphosphino)hexane (dpph), [(dpph-*P*,*P*′)Ag(μ-SCN)$_2$Ag(*P*,*P*′-dpph)] (Effendy *et al.*, 2005). The monoclinic form of [(dpph-*P*,*P*′)Ag(μ-SCN)$_2$Ag(*P*,*P*′-dpph)] was found to be isomorphous with [(dppb-*P*,*P*′)Ag(μ-CN)$_2$Ag(*P*,*P*′-dppb)] prepared from 1,4-bis(diphenylphosphino)butane (dppb; Effendy *et al.*, 2005). Each of the Ag atoms in both polymorphs and in the related compounds has a distorted tetrahedral geometry (Table 3) with two terminal tris(*p*-fluorophenyl)phosphine ligands and with an S atom and an N atom from the two bridging thiocyanate ligands. In this arrangement the P—Ag—P angle, as in most other silver(I) complexes with a tetrahedral geometry around the Ag atom, is enlarged to almost 120°, and even larger in (III) [126.13 (3)°] and (VI) [124.66 (4)°]. In all molecules of the two polymorphs, one of the two P—Ag—N angles is smaller (ranges between 92 and 95°), while the other is larger (and ranges between 106 and 117°) compared with the P—Ag—S angle (ranges between 110 and 117°). The bond distances are also listed in Table 2 and also correspond to those of complexes (III)–(VI) (Venter *et al.*, 2007; Effendy *et al.*, 2005; Bowmaker *et al.*, 1997).

Crystal densities are sometimes taken to indicate which polymorph is more stable. In this case equal densities for the two polymorphs [(I) being just 0.003 Mg m$^{-3}$ less dense than (II)] indicate that the stability of the two is comparable. This is not surprising given that the two were grown from the same solvent under the same conditions. This is also an indication of equal effective packing (see also Fig. 5). However, a look at the cavities in the structures (Spek, 1990) of the two polymorphs shows they are different with (I) having less cavities (four in the unit cell with a radius of 1.088 Å) than (II) (16 in the unit cell – 10 with a radius of 1.202 and 6 with a radius of 1.039 Å). In addition, the simulated powder patterns of the two polymorphs are significantly different (see supplementary material).

In the structures of the two polymorphs, C—H$\cdots\pi$ intermolecular interactions and C—H$\cdots$F inter- and intramolecular interactions seem to play a vital role in their packing patterns. Table 4 lists some of the interactions found in the two structures. In polymorph (I) molecules are connected to one another through C—H$\cdots\pi$ intermolecular interactions [C225—H225$\cdots$Cg, C$\cdots$Cg = 3.622 (3) Å, symmetry operator: $x+1, y, z$] on one side and through C—H$\cdots$F intermolecular interactions [C215—H215$\cdots$F23, C$\cdots$F = 3.448 (3) Å, symmetry operator; $x-1, y, z$] on another along the crystallographic *a* direction. Two other C—H$\cdots$F interactions [C216—H216$\cdots$F22 and C222—H222$\cdots$F11, symmetry

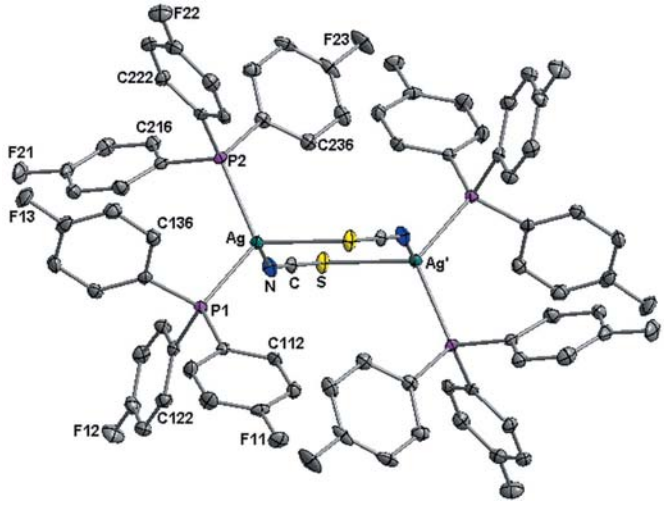


**Figure 3**
The numbering scheme for polymorph (I) at 100 K. The displacement ellipsoids are drawn at 50% probability. The symmetry operator for generating the second half of the molecule is: $-x, 1-y, -z$.

operators; $-\frac{1}{2}+x,\frac{1}{2}-y,\frac{1}{2}+z$ and $-\frac{1}{2}-x,\frac{1}{2}+y,\frac{1}{2}-z$] on either sides of a molecule complete the packing connecting to other molecules through an *n*-glide relation.

Polymorph (II) has phenyl rings located close to each other resulting in five C—H···$\pi$ interactions (see Table 4). Three of these interactions participate in connecting the two independent molecules in the asymmetric unit [(ii) C315—H315···$\pi$, (iii) C435—H435···$\pi$ and (iv) C533—H533···$\pi$, symmetry operator = $-x+1,-y+1,-z$]. This is in addition to three C—H···N intramolecular interactions involving the three N atoms from both molecules in the asymmetric unit. In addition to C—H···$\pi$ and C—H···F intermolecular interactions, polymorph (I) has S···S interactions in its crystal structure, 0.13 Å shorter than the sum of van der Waals radii of two S atoms [S···S = 34650 (9) Å, symmetry operator = $-1+x,y,z$] connecting molecules along the crystallographic *a* axis. The presence of the second molecule in polymorph (II) is probably a reason for the absence of S···S interactions in its crystal structure. In the structure of (II) the two molecules are connected in an alternating manner leading to chains that run diagonally through the body of the unit cell. In all, these interactions are responsible for the different packing arrangements of molecules in the crystals of the two polymorphs, hence the difference in the orientation of the *p*-fluorophenyl rings.

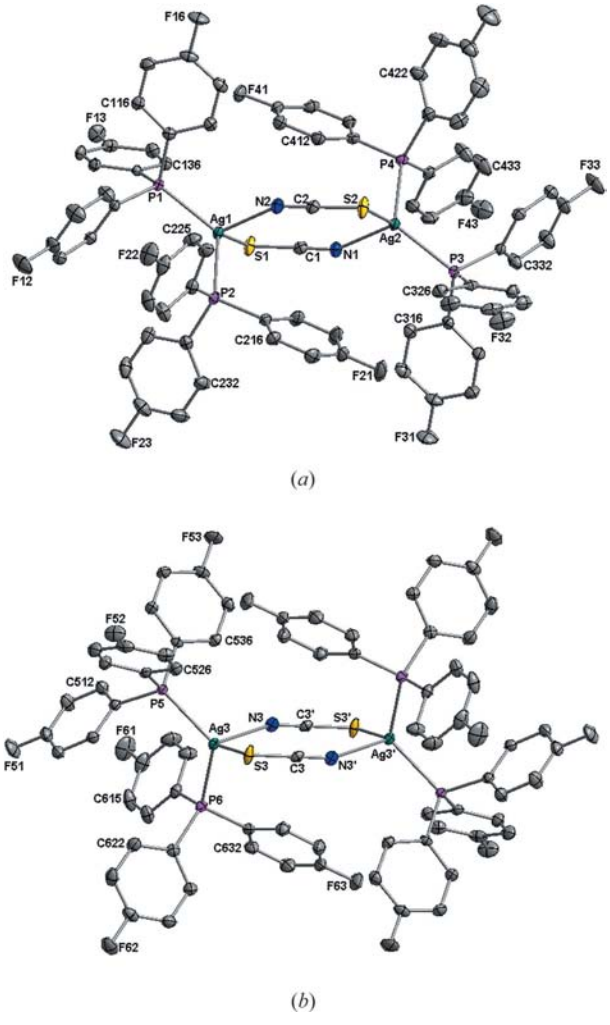


**Figure 4**
The numbering scheme for polymorph (II) at 100 K, (*a*) the full molecule and (*b*) the half molecule; both in the asymmetric unit. The displacement ellipsoids are drawn at 50% probability. Symmetry operator for generating the second half of (II*b*) is: $-x,2-y,1-z$.

**Table 4**
C—H···$\pi$, C—H···F and C—H···N intermolecular interactions for polymorphs (I) and (II).

| | C—H···$\pi$ | H···$\pi$ | ∠C—H···$\pi$ | C···$\pi$ |
|---|---|---|---|---|
| (I) | C225$^{i}$—H225···$\pi$ | 2.72 | 158 | 3.622 (3) |
| (II) | C225$^{ii}$—H225···$\pi$ | 2.79 | 157 | 3.658 (2) |
| | C315$^{iii}$—H315···$\pi$ | 2.94 | 171 | 3.865 (2) |
| | C435$^{iv}$—H435···$\pi$ | 2.74 | 150 | 3.578 (2) |
| | C533$^{v}$—H533···$\pi$ | 2.91 | 161 | 3.863 (2) |
| | C535$^{vi}$—H535···$\pi$ | 2.84 | 174 | 3.766 (2) |

Symmetry operators: (i) $1+x,y,z$; (ii) $1-x,\frac{1}{2}+y,\frac{1}{2}-z$; (iii)–(v) $1-x,1-y,-z$; (vi) $1-x,-y,-z$.

| | C—H···*X* | *D*—H | H···*A* | *D*···*A* | *D*—H···*A* |
|---|---|---|---|---|---|
| (I) | C215$^{i}$—H215···F23 | 0.95 | 2.51 | 3.448 (3) | 168 |
| | C216$^{ii}$—H216···F22 | 0.95 | 2.51 | 3.275 (3) | 138 |
| | C222$^{iii}$—H222···F11 | 0.95 | 2.43 | 3.213 (3) | 140 |
| (II) | C112$^{iv}$—H112···N2 | 0.93 | 2.47 | 3.382 (2) | 16 |
| | C223$^{v}$—H223···F63 | 0.93 | 2.44 | 3.246 (2) | 146 |
| | C316$^{vi}$—H316···N1 | 0.93 | 2.6 | 3.527 (2) | 175 |
| | C425$^{vii}$—H425···F22 | 0.93 | 2.55 | 3.272 (3) | 135 |
| | C433$^{viii}$—H433···F41 | 0.93 | 2.5 | 3.206 (3) | 132 |
| | C536$^{ix}$—H536···N3 | 0.93 | 2.4 | 3.331 (2) | 175 |
| | C615$^{x}$—H615···F21 | 0.93 | 2.41 | 3.212 (2) | 145 |

Symmetry operators: (i) $-\frac{1}{2}-x,-\frac{1}{2}+y,\frac{1}{2}-z$; (ii) $1+x,y,z$; (iii) $-\frac{1}{2}+x,-\frac{1}{2}-y,\frac{1}{2}+z$; (iv) intramolecular; (v) intramolecular; (vi) intramolecular; (vii) $1-x,-\frac{1}{2}+y,\frac{1}{2}-z$; (viii) $2-x,-\frac{1}{2}+y,\frac{1}{2}-z$; (ix) intamolecular $-x,1-y,-z$; (x) $x,1+y,z$.

In the crystal of polymorph (II), molecule (II*A*) is situated at $(1/3,\frac{1}{2},1/3)$ while (II*B*) is at $(0,1,\frac{1}{2})$ from the origin. The two molecules are related by pseudo-translation described by the criteria, rotation by 0.25 Å, inversion by 0.45 Å and translation by 0.45 Å.

### 3.3. Structural comparison of polymorphs (I) and (II) using r.m.s. and half-normal probability analysis

An r.m.s. error calculation is one way to compare similar structures and can also show clear differences on certain parts of two or more molecules in comparison. The calculated r.m.s. error between polymorph (I) and (II) is 4.37 Å, which is rather large but is also a clear indication of the geometric differences between the two polymorphs as manifested in the overlay of the two structures (Fig. 6). It is clear from this overlay that there are extreme differences in the orientations of the *para*-fluorophenyl rings, hence the large r.m.s. error.

Ordered weighted differences between matching parameters in independently determined structures follow a Gaussian distribution only if both determinations are subject to the influence of random effects. Departures from Gaussian are readily detectable by plotting experimental deviates against the corresponding normal probability deviates

(Abrahams & Keve, 1971; Abrahams, 1997). De Camp (1973) suggested that interatomic distances can be used as chemical coordinates. The technique can be used as a quantitative companion to r.m.s. error calculations which identifies the exact differences in geometric parameters between two structures. Additional information can be found in the supplementary material.

Figs. 7(*a*) and (*b*) show half-normal probability plots for a comparison between polymorph (I) and polymorph (II). Fig. 7(*a*) shows dependent bond distances of the two polymorphs, whereas Fig. 7(*b*) shows comparison for data sets of the independent bond distances. Interatomic distances with largest $\delta m_i$ for the two polymorphs are presented in Table 5. With 48 non-H atoms in each of the two polymorphs, there are 138 interatomic independent distances ($3n - 6$). These distances represent the direct bond lengths (53; first order), bond angles (59; second order) and torsion angles (26; third order distances). Most of the systematic differences between the two structures are of second or third order and are of distances involving the Ag and P atoms, as well as the orientation of the *p*-fluorophenyl rings. The largest differences are observed in the torsion angles around Ag—C126, Ag—C226 and Ag—C116 and in the angle Ag—C111. This is related to differences of the two polymorphs as observed in the overlay picture in which corresponding *p*-fluorophenyl rings have different orientations.

**Table 5**
Interatomic distances with largest $\delta m_i$ for the two polymorphs.

| $\delta m_i$ | Distance | Order |
|---|---|---|
| 2.50 | Ag—C216 | 3 |
| 2.75 | C1—P1 | 3 |
| 2.88 | Ag—C121 | 2 |
| 2.97 | Ag—C211 | 2 |
| 3.73 | Ag—C136 | 3 |
| 4.08 | Ag—C236 | 3 |
| 4.27 | N2—P1 | 2 |
| 6.03 | Ag—C111 | 2 |
| 6.10 | Ag—C126 | 3 |
| 23.30 | Ag—C226 | 3 |
| 25.43 | Ag—C116 | 3 |

Fig. 7(*b*) shows non-linear behaviour with intercepts that are much less than one for the independent distances. This is an indication that there are major systematic geometric differences between polymorph (I) and polymorph (II). This plot (Fig. 7*b*) shows linearity to only $\alpha_i = 0.95$ with an intercept much less than 1 and a slope of 0.72 (−0.5476, $R = 0.9545$). This analysis of the independent distances confirms that the molecular structures of the two polymorphs are significantly different. Again we can safely attribute this non-linearity to the completely different orientations of the *p*-fluorophenyl rings of the two polymorphs.

## 4. Conclusions

The two polymorphs of title compound di-$\mu$-thiocyanato-$\kappa^2N$:$S$;$\kappa^2S$:$N$-bis[bis(tri-*p*-fluorophenylphosphine-$\kappa P$)silver(I)] were crystallographically determined and are reported. Both have similar densities and this agrees with their behaviour as concomitant polymorphs. The two polymorphs are structurally compared using half-normal probability plot analyses, as well

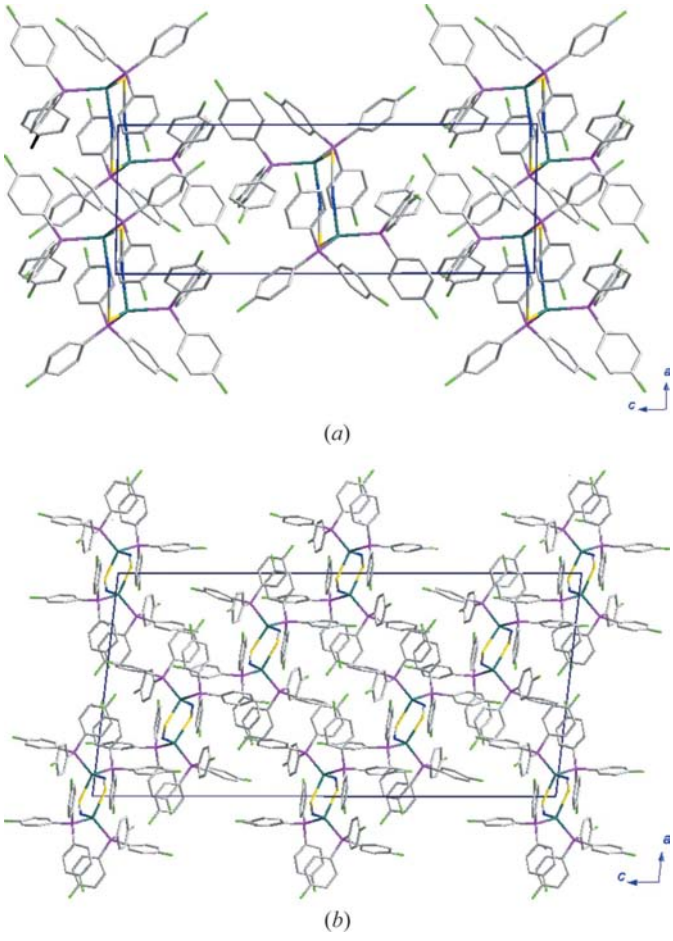


**Figure 5**
(*a*) Packing of polymorph (I) and (*b*) packing of polymorph (II), as viewed down the crystallographic *b* axis.

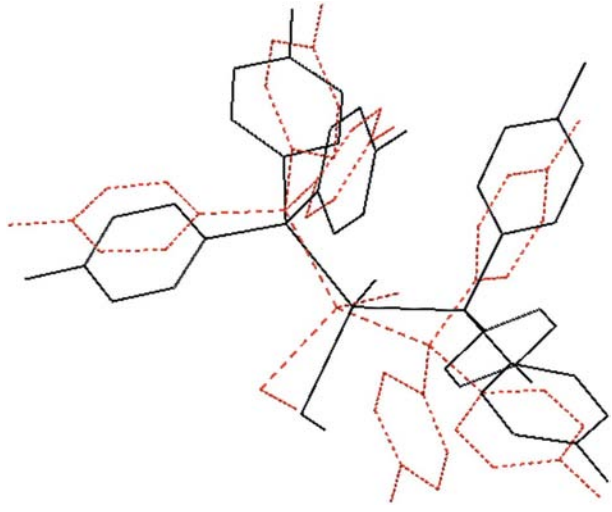

**Figure 6**
Overlay of polymorph (I) and the second molecule of polymorph (II).

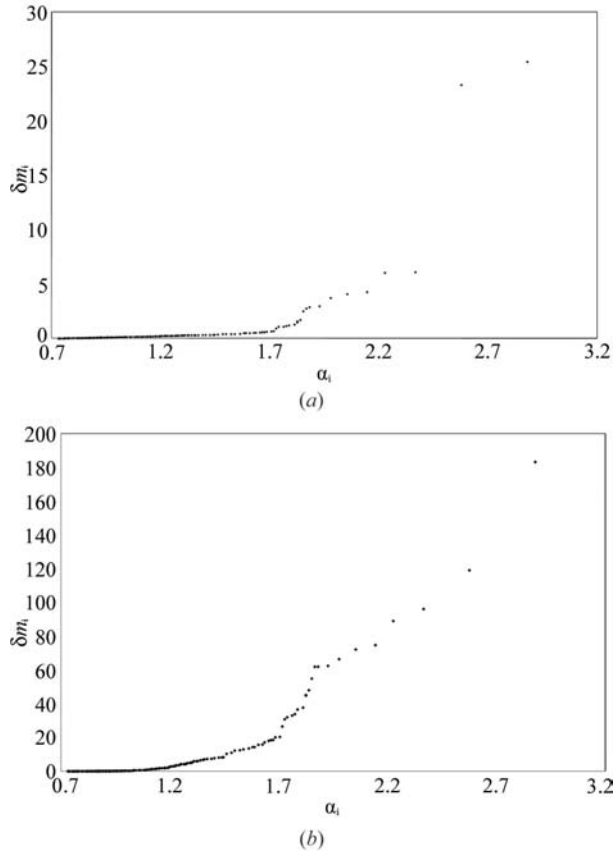


**Figure 7**
Half-normal probability plots (non-H bond lengths and angles used) comparing (*a*) dependent distances and (*b*) independent distances, between polymorph (I) and polymorph (II) at 100 K.

as r.m.s error calculations. The r.m.s. error is rather large and due to the major differences in the orientations of the *p*-fluorophenyl rings. Both the r.m.s. error and the intercepts of the h.n.p. plot of independent distances are indicative of major structural differences, most of which are of second and third order, *i.e.* related to torsion angles involving the Ag metal and the phosphine groups.

Financial assistance from the Research Fund of the University of Johannesburg gratefully acknowledged. Part of this material is based on work supported by the South African National Research Foundation. Opinions, findings, conclusions or recommendations expressed in this material are those of the authors and do not necessarily reflect the views of the NRF. Dr A. J. Muller and Dr J. M. Janse van Rensburg (University of Free State) are acknowledged for collection of the X-ray data.

## References

Abrahams, S. C. (1997). *Acta Cryst.* A**53**, 673–675.
Abrahams, S. C. & Keve, E. T. (1971). *Acta Cryst.* A**27**, 157–165.
Albertsson, J. & Schultheiss, P. M. (1974). *Acta Cryst.* A**30**, 854–855.
Allen, F. H. (2002). *Acta Cryst.* B**58**, 380–388.
Altomare, A., Burla, M. C., Camalli, M., Cascarano, G. L., Giacovazzo, C., Guagliardi, A., Moliterni, A. G. G., Polidori, G. & Spagna, R. (1999). *J. Appl. Cryst.* **32**, 115–119.
Bowmaker, G. A., Effendy, Hart, R. D., Kildea, J. D., De Silva, E. N. & White, A. H. (1997). *Aust. J. Chem.* **50**, 627–640.
Bowmaker, G. A., Effendy, Harvey, P. J., Healy, P. C., Skelton, B. W. & White, A. H. (1996). *J. Chem. Soc. Dalton Trans.* pp. 2449–2457.
Brandenburg, K. & Putz, H. (2005). *DIAMOND*, Version 3.0c. Crystal Impact GbR, Bonn, Germany.
Bruker (2003). *COSMO*, Version 1.48. Bruker AXS Inc., Madison, Wisconsin, USA.
Bruker (2004). *SAINT-PLUS*, Version 7.12, *XPREP* and *SADABS*, Version 2004/1. Bruker AXS Inc., Madison, Wisconsin, USA.
Bruker (2005). *APEX*2, Version 1.0–27. Bruker AXS Inc., Madison, Wisconsin, USA.
De Camp, W. H. (1973). *Acta Cryst.* A**29**, 148–150.
Effendy, Di Nicola, C., Fianchini, M., Pettinari, C., Skelton, B. W., Somers, N. & White, A. H. (2005). *Inorg. Chim. Acta*, **358**, 763–795.
Farrugia, L. J. (1999). *J. Appl. Cryst.* **32**, 837–838.
Hansson, C., Lindqvist, M. & Oskarsson, Å. (2008). *Acta Cryst.* B**64**, 187–195.
Howatson, J. & Morosin, B. (1973). *Cryst. Struct. Commun.* **2**, 51.
Hypercube Inc. (2002). *HyperChem*, Version 7.52. Hypercube Inc., Florida, USA.
Mann, F. G., Wells, A. F. & Purdue, D. (1937). *J. Chem. Soc.* pp. 1828–1836.
Meijboom, R. (2006). *Acta Cryst.* E**62**, m2698–m2700.
Meijboom, R. (2007). *Acta Cryst.* E**63**, m78–m79.
Meijboom, R., Bowen, R. J. & Berners-Price, S. J. (2009). *Coord. Chem. Rev.* **253**, 325–342.
Meijboom, R. & Muller, A. (2006). *Acta Cryst.* E**62**, m3191–m3193.
Meijboom, R., Muller, A. & Roodt, A. (2006). *Acta Cryst.* E**62**, m2162–m2164.
Microsoft (2003). *EXCEL*. Microsoft Inc., USA.
Muetterties, E. L. & Alegranti, C. W. (1972). *J. Am. Chem. Soc.* **94**, 6386–6391.
Sheldrick, G. M. (2008). *Acta Cryst.* A**64**, 112–122.
Spek, A. L. (1990). *Acta Cryst.* A**46**, C34.
Teo, B.-K. & Calabrese, J. C. (1976*a*). *Inorg. Chem.* **15**, 2467–2474.
Teo, B.-K. & Calabrese, J. C. (1976*b*). *Inorg. Chem.* **15**, 2474–2486.
Venter, G. J. S., Meijboom, R. & Roodt, A. (2006). *Acta Cryst.* E**62**, m3453–m3455.
Venter, G. J. S., Meijboom, R. & Roodt, A. (2007). *Acta Cryst.* E**63**, m3076–m3077.
Venter, G. J. S., Meijboom, R. & Roodt, A. (2009). *Inorg. Chim. Acta*, **362**, 2475–2479.
Venter, G. J. S., Roodt, A. & Meijboom, R. (2009). *Acta Cryst.* B**65**, 182–188.